ADVANCED ROCKET ENGINE CRYOGENIC TURBOPUMP BEARING THERMAL MODEL

Joe C. Cody, Linda New, Bruce Tiller
Aerospace Systems & Products Division
Spectra Research Systems, Huntsville Division

Abstract

A lumped node thermal model has been developed representing the Space Shuttle Main Engine (SSME) liquid oxygen (LOX) turbopump turbine end bearings operating in a cryogenically cooled bearing tester. Bearing elements, shaft, carrier, housing, cryogen flow characteristics, friction heat, and fluid viscous energy are included in the model. Heat transfer characteristics for the regimes of forced convection boiling are modeled for liquid oxygen (LOX) and liquid nitrogen (LN_2). Large temperature differences between the cryogenic fluid and bearing contact surfaces require detailed nodal representation in these areas. Internal loads and friction heat are affected by temperature dependent operating clearances requiring iterations between bearing thermal and mechanical models. Results compare favorably with limited data from the Marshall Space Flight Center (MSFC) Bearing Materials Tester (BMT). Analyses indicate a thermal-mechanical coupling resulting in reduced operating clearances, increased loading and heating which can contribute to premature bearing failure. Contact surfaces operate at temperatures above local saturation resulting in vapor rather than liquid in the contacts, precluding possible liquid film lubrication. Elevated temperatures can reduce lubrication, increase friction, and reduce surface hardness supporting a surface failure mode rather than subsurface fatigue. Future efforts include modeling the SSME liquid hydrogen turbopump bearings, model refinements, and further correlation of modeling techniques with BMT data.

Introduction

This thermal modeling development supports an overall MSFC Bearing Materials evaluation program designed to formulate and experimentally verify failure modes and life prediction models for high speed rolling bearings operating in cryogens. This research supports development and improvement of hardware such as the Space Shuttle Main Engine liquid oxygen (LOX) and liquid hydrogen (LH_2) turbopumps which are highly efficient lightweight machines operating at high power levels and shaft speeds. The pump main shafts are supported by angular contact ball bearings operating in the cryogen being pumped.

State of the art bearing codes are not adequate for thermal simulation of high speed rolling bearings operating in cryogens. Although sufficient for analysis of conventionally lubricated bearings, treatment of the various regimes of boiling, large temperature gradients, and significant variations in material properties is beyond the scope of these codes. The current thermal modeling effort is directed toward improved treatment of these important characteristics of cryogenic bearing systems, and to provide a better understanding of the thermal influences on cryogenic bearing operating characteristics and life. Objectives are to develop and refine the bearing model, correlate results with BMT data, and provide a verified design tool for predicting the thermal characteristics of high speed rolling bearings operating in cryogens.

Approach

Model Description

A state of the art thermal code "SINDA" was selected for modeling the cryogenic bearing system. This code has the capability for temperature and time varying boundary conditions, and temperature varying material properties. It also provides for modeling of fluid networks which is necessary to simulate the cryogenic fluid flow. The internal arrangement of

the BMT is shown in Figure 1. Since the right and left bearing pairs are essentially similar, only one bearing pair requires modeling. The cryogen, acting as a coolant, enters a manifold at each end of the tester, flows through each bearing and exits via a common flow path. Although the tester can be loaded in both the axial and radial directions, the current computer simulation treats only the axially loaded case. Since this produces axially symmetric loading a radial slice of the system is all that requires modeling. Figure 2, a schematic of the bearing set, illustrates a representative radial section of the model. The bearing is a 57 mm bore angular contact ball bearing with thirteen balls.

Due to the large temperature differences in the bearing contact surfaces and cryogenic fluid, large thermal gradients are present in the balls and races near the highly loaded contacts. This, in addition to the extreme sensitivity of the fluid heat transfer coefficient to surface temperature, required many very small nodes in the contact areas of the model. The nodal representation of the inner race, ball, and outer race for the 57 mm LOX pump turbine end bearing is shown in Figure 3. There are 642 nodes in the model. Surface nodes are connected by appropriate thermal resistors to the cryogenic fluid. These resistors are varied as the surface temperature of the node changes to represent the appropriate fluid heat transfer regime. The ball contacts the inner and outer races in a small elliptical area that varies in size and location with speed and load. The detailed nodal representation allows flexibility to account for these variations without renoding the model.

Fluid Heat Transfer Coefficients

Wide variations in component surface temperatures carries the fluid heat transfer mechanisms through the range of forced convection in liquid, high velocity forced convection boiling, and forced convection in vapor. Since test data are absent for high velocity, high pressure forced convection

boiling of cryogens, a superposition method [2] was used to evaluate the appropriate flow regimes depending on the surface superheat.

Figure 4 provides a graphical illustration of the method for evaluating the heat transfer regimes as a function of surface superheat for LN_2. As shown, when the forced convection heat flux equals the nucleate boiling flux incipient boiling is assumed to occur. As the surface superheat exceeds about 3.3°R the surface is assumed to be vapor blanketed and forced convection vapor is the mode of heat transfer. Since this indicates about an order of magnitude reduction in heat transfer, the significance of the superheat value at which transition occurs becomes apparent. Heat fluxes for the different regimes were calculated from the following equations-the Dittus-Boelter equation for forced convection on all components except the balls, Katsnellson's equation for forced convection on the balls, the Borishanskiy-Minchenko correlation for nucleate boiling, and the Kutateladze correlation for the peak heat flux.[2] This technique was tentatively verified with tester data as illustrated in Figure 5, where a comparison of predicted and measured bearing outer race temperatures is shown. The predicted values are provided as a function of surface superheat and indicate that a superheat range of 2 to 6 degrees provides reasonable agreement with the measured BMT test data. A similar analysis was conducted for LOX^2.

Heat Generated by Friction in the Bearing Contact Area

Heat is generated in the raceway contacts due to ball spin and roll. Additional frictional heat, not yet included in the model, is generated by the ball contacting the cage, and the cage contacting the inner surface of the outer raceway. The cage effects are in the process of being incorporated into the model.

The raceway frictional heat generated is obtained from the SHABERTH[3] bearing code. This code also provides bearing operating characteristics such as contact angles, operating clearances, contact stresses, deflections, ball and cage speeds and bearing reactions. Shown in Figure 6 is an example of the frictional heat generated in the inner race contacts for the conditions noted. The two minimum points indicate the areas of ball roll and the maximum value is caused by the high relative velocities due to ball spin. Similar information may be generated for the outer race. These values are used as input to the bearing thermal model.

Heat Generated by Mechanically Working the Fluid

Considerable heat is generated in the shaft bearing system due to mechanical work on the coolant fluid. Heat generated from fluid stirring and friction was estimated[4] for each component. A BMT heat balance provided a measure of the total heat into the system. Estimated values were adjusted to match the BMT heat balance. The estimated values were from 45% to 80% too low with the larger deviation at the lower shaft speeds. Results are shown in Figure 7. Included are values of contact frictional heat for the loading conditions shown. This data illustrates the large percentage of heat input to the system from fluid work.

Thermal Model Results

Results of the bearing thermal model show high local temperatures and steep temperature gradients in the ball/race contact areas. Examples are shown in Figures 8, 9 and 10. Figure 8 illustrates representative surface temperatures and gradients in the ball. There is a wide variation in surface temperature, and much of the surface is above the local saturation temperature (-241°F) of the LN_2 coolant. Inner race temperatures are shown in Figure[2] 9. These surface temperatures are also above the local fluid saturation temperature as are most of the outer race track nodes shown in Figure 10. These temperatures

show that for the conditions analyzed the bearing contacts are operating in vapor rather than liquid. In addition, the maximum temperature shown in the ball track (461°F) is approaching temperatures that can affect surface hardness of the 440C steel.

Thermal-Mechanical Interactions

The inner races of high speed rolling bearings reach a higher operating temperature than the outer races because of the increased ball spin at the inner race. This causes inner race growth relative to the outer race and has the effect of increasing loads and reducing internal operating clearances and contact angles. If bearing clearances and/or cooling capacity is marginal, this effect can amplify causing increased loading and heating and possible premature bearing failure. Examples of this trend are shown in Figures 11 and 12. Figure 11 shows the reduction in internal clearance as the coolant flow is decreased, and Figure 12 shows the corresponding increase in component temperature.

Comparison of Model and Test Results

Shown in Figure 13 are comparisons of the measured and calculated outer race temperature and the coolant outlet temperature. These results show fair agreement between the measured temperatures and model predictions even though a slight difference in coolant flow rate exists because the thermal model predictions were conducted well before the actual test run and at that time the flow rates were not precisely known. BMT test data is limited at this time. As additional test data becomes available further verification and/or model refinements will be made.

Conclusions

Development of a bearing thermal model capable of accounting for two-phase cryogenic flow characteristics has revealed unexpected high temperatures in the loaded contacts. These contact areas operate

at temperatures well above the local saturation temperature and are operating in a vapor rather than liquid environment. The lubrication benefits that might be expected from a liquid film separating the contacts does not occur. For some loading and coolant flow conditions, the model shows that there is a thermal-mechanical coupling that can cause loss of operating clearances, increased loading, and increased heat generation that can contribute to premature bearing failure. Elevated temperatures can reduce lubrication, increase friction, and reduce surface hardness. These conditions support a surface failure mode rather than the subsurface fatigue experienced by conventional oil lubricated rolling bearings.

Bearing modeling techniques are providing valuable tools for the assessment of new materials for high speed bearings operating in cryogens. However, due to the complexity of the system and lack of experimental data in many areas, especially high flow two-phase cryogenic heat transfer characteristics, additional data from the MSFC BMT is vital for verification of cryogenic bearing systems modeling methods.

References

1. SINDA Engineering Program Manual (Contract No. NAS9-10435) June 1971.

2. Bearing Tester Data Compilation, Analysis, and Reporting and Bearing Math Modeling (Contract No. NAS8-34686), May 1984, Final Report.

3. SHABERTH Computer Program Operation Manual, Technical Report AFAPL-TR-76-90, October 1976.

4. NASA Report No. 793, "Experiments on Drag of Revolving Disks, Cylinders, and Streamline Rods at High Speeds", by T. Theodorsen and A. Regier.

FIGURE 1 SHAFT, BEARINGS & CARRIER APPLIED LOADS

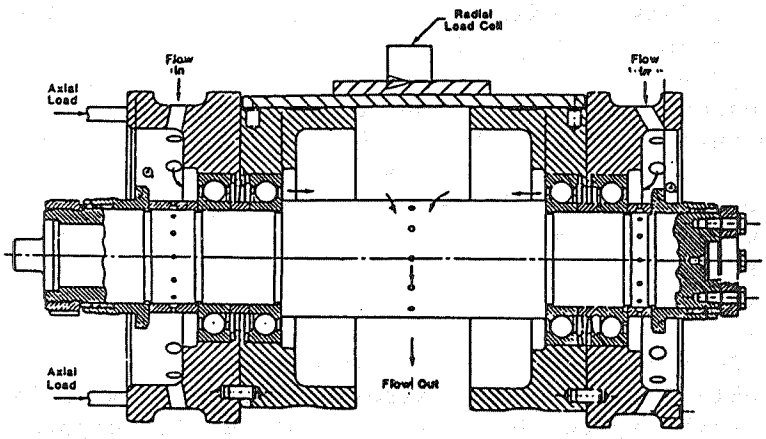

FIGURE 2 SCHEMATIC OF BEARING SET

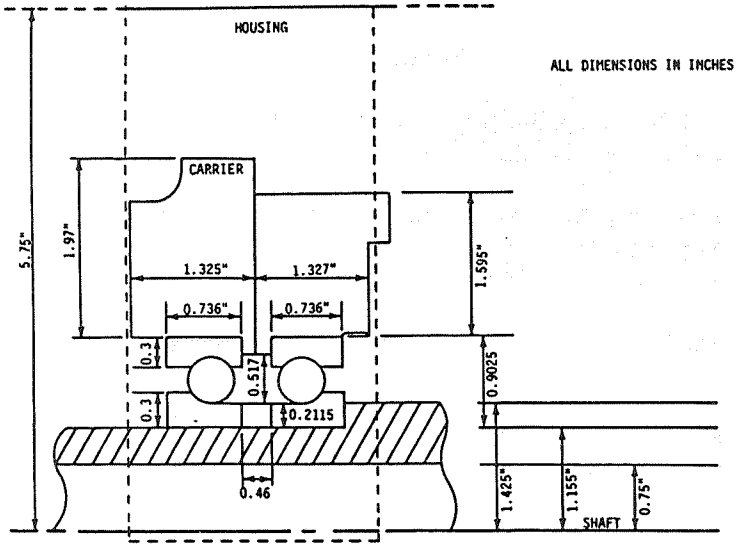

FIGURE 3 DETAILED NODAL REPRESENTATION OF 57mm BEARING

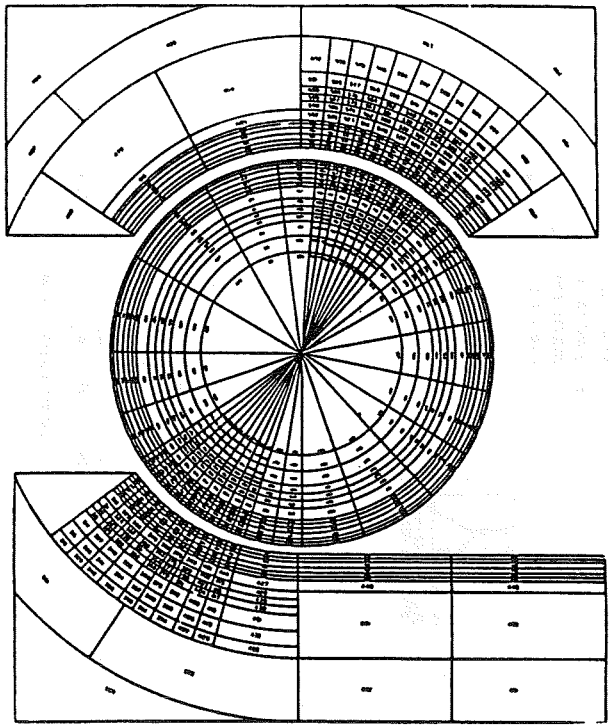

FIGURE 4 HEAT TRANSFER REGIMES FOR LN_2

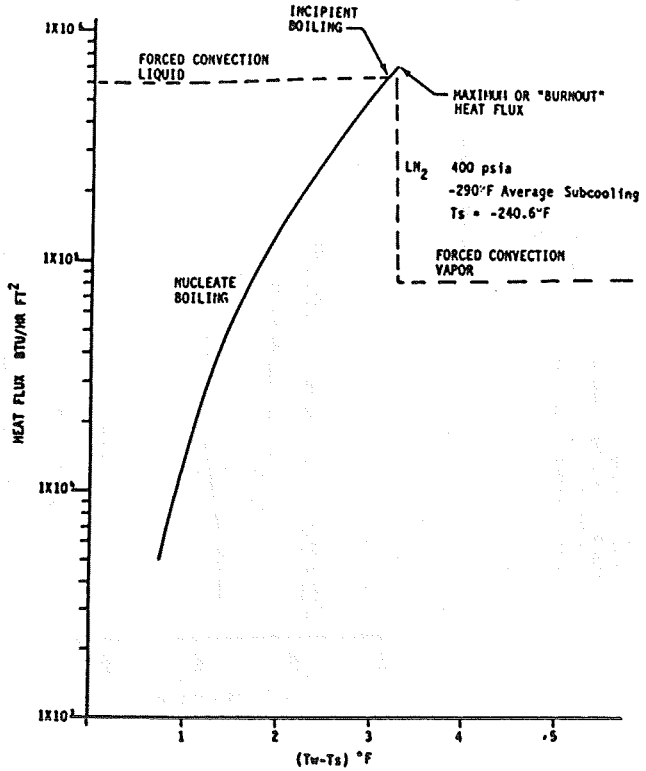

FIGURE 5 Outer Race Node Temperature As A Function of Hall Superheat at Max Flux Conditions (LOX Turbopump Turbine End Bearing - 57 mm)

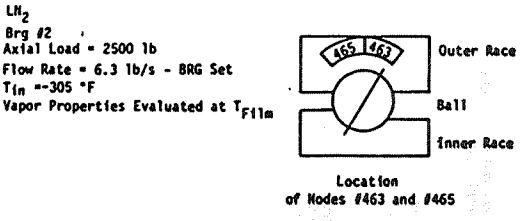

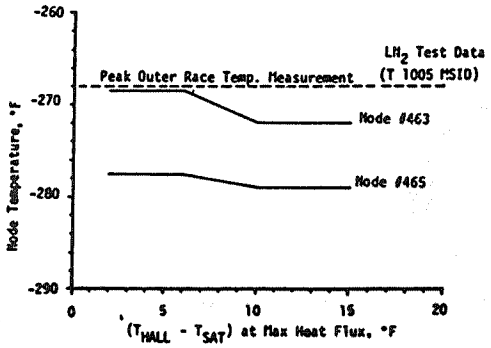

FIGURE 6 INNER RACE HEAT GENERATED AT CONTACT ELLIPSE

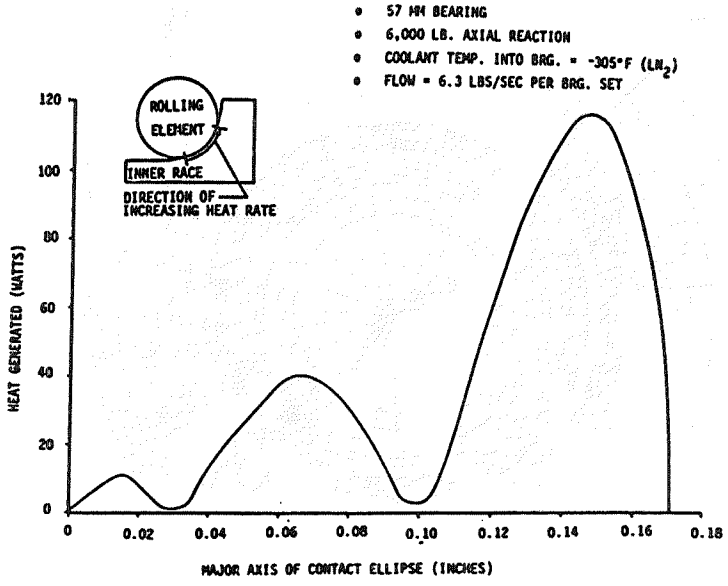

FIGURE 7
HEAT GENERATED (KW) AT LOAD END OF THE BMT AS A FUNCTION OF SHAFT SPEED AND AXIAL LOAD (LN_2 COOLANT)

COMPONENT LOADS(LBS)	SHAFT SPEED (RPM)							
	15,000		20,000		25,000		30,000	
	2500	4000	2500	4000	2500	4000	2500	4000
SLINGER	3.11	3.11	7.1	7.1	11.2	11.2	17.84	17.84
SPACER	1.18	1.18	2.7	2.7	4.45	4.45	6.87	6.87
SHAFT	4.0	4.0	9.15	9.15	15.	15.	23	23
BGR #1								
VISCOUS	5.77	5.77	14.	14.	23.	23.	40.2	40.2
FRICTION	.40	.40	.72	.72	1.12	1.12	1.9	1.9
BGR #2								
VISCOUS	1.17	1.17	2.66	2.66	4.38	4.38	7	7
FRICTION	2.42	4.48	3.64	6.44	5.29	8.86	7.3	11.5
TOTAL	18.	20.	40.	42.8	64.4	68.2	104.1	108.3

FIGURE 8 TEMPERATURE -VS- DEPTH BELOW SURFACE OF ROLLING ELEMENT

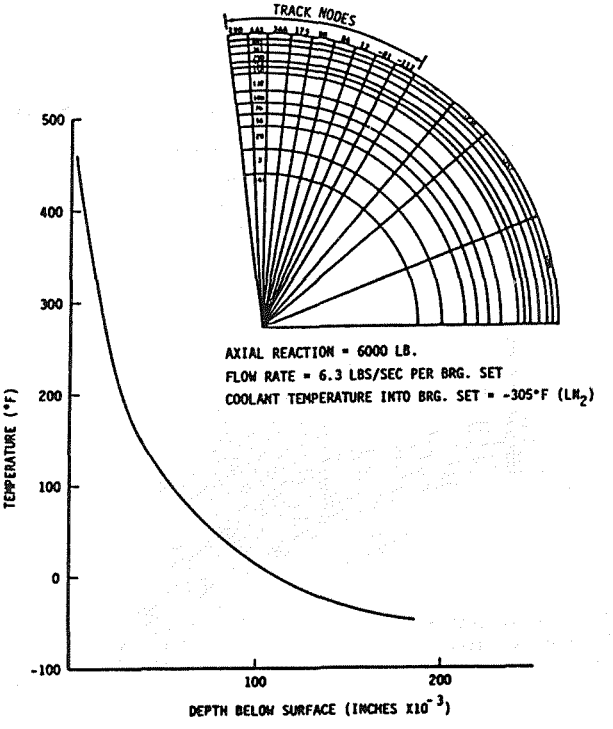

FIGURE 9 INNER RACE TEMPERATURE DISTRIBUTION FOR LOX PUMP TURBINE END BEARING

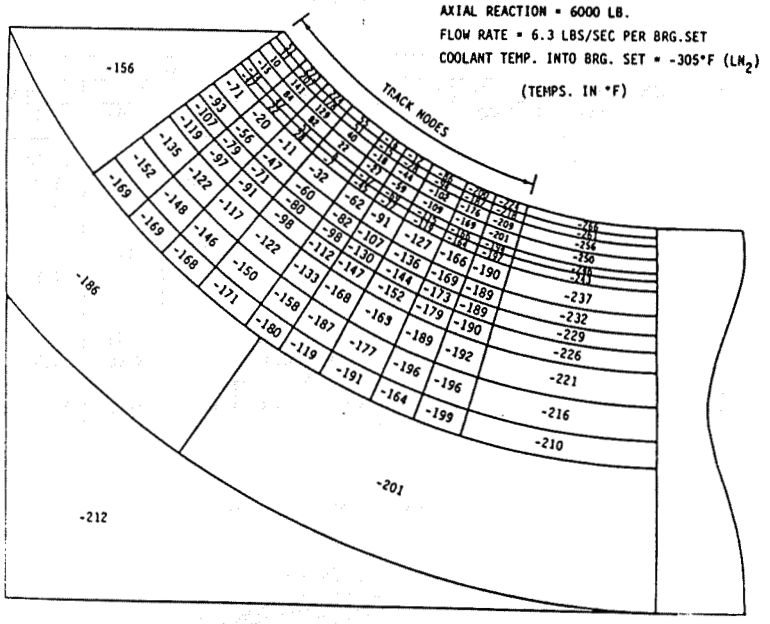

FIGURE 10 OUTER RACE TEMPERATURE DISTRIBUTION FOR LOX PUMP TURBINE END BEARING

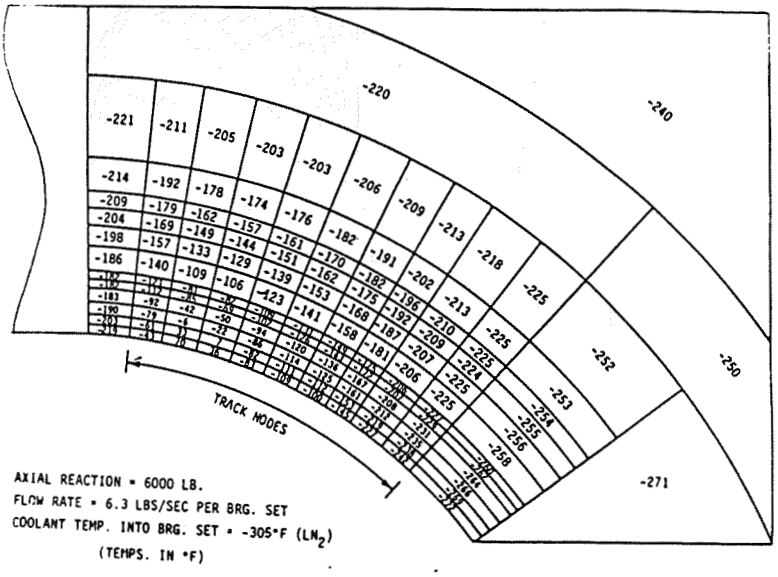

FIGURE 11 OPERATING CLEARANCE VS COOLANT FLOW

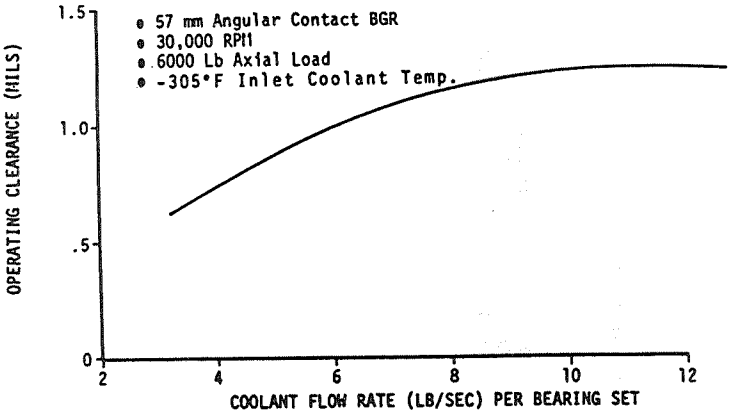

FIGURE 12

AVERAGE BEARING COMPONENT TEMPERATURE VS COOLANT FLOW

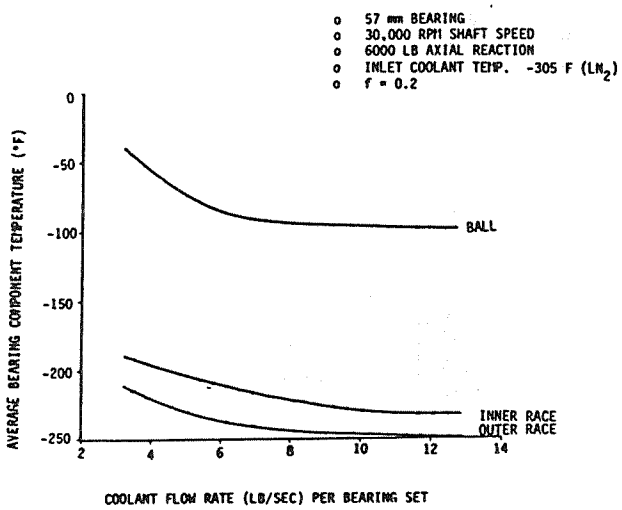

FIGURE 13
COMPARISON OF MODEL PREDICTIONS AND TEST RESULTS

OPERATING PARAMETERS	BEARING THERMAL MODEL RESULTS RUN DATE 9-29-83	BEARING MATERIALS TESTER DATA TEST DATE 4-26-84 TEST # 201N0409	BEARING MATERIALS TESTER DATA TEST DATE 5-15-84 TEST # 201N0501
SHAFT SPEED (RPM)	25,000	25,000	25,000
LN_2 COOLANT FLOW RATE (LB/SEC PER BRG. PAIR)	6.0	6.4	6.3
INLET COOLANT TEMPERATURE (°F)	-300	-300.5	-296
COOLANT TEMPERATURE OUT OF LOADED BEARING (°F)	-283.8	-281.5	-275
OUTER RACE BEARING TEMPERATURE (°F)	-278.2	-279	-276

FIGURE 14
COMPARISON OF MODEL PREDICTIONS AND TEST RESULTS

OPERATING PARAMETERS	BEARING THERMAL MODEL RESULTS RUN DATE: 11-10-83	BEARING MATERIALS TESTER DATA LN_2 ROTATION 82-62-17-40-12-121
SHAFT SPEED (RPM)	30,000	30,000
LN_2 COOLANT FLOW RATE (LB/SEC PER BRG. PAIR)	6.3	6.3
INLET COOLANT TEMPERATURE (°F)	-305	-303
COOLANT TEMPERATURE OUT OF LOADED BEARING (°F)	-275.1	-274
OUTER RACE BEARING TEMPERATURE (°F)	-268.5	-269